ORNL/TM-2019/1454

Determination Of Stress-Free Lattice Spacing (D_0) For Residual Stress Relaxation Measurement In Ni-Based Superalloys By Neutron Diffraction

Yan Chen
Ke An
Alexandru D. Stoica

May 11th, 2020

OAK RIDGE NATIONAL LABORATORY
MANAGED BY UT-BATTELLE FOR THE US DEPARTMENT OF ENERGY

ORNL/TM-2019/1454

Neutron Scattering Division

DETERMINATION OF STRESS-FREE LATTICE SPACING (D_0) FOR RESIDUAL STRESS RELAXATION MEASUREMENT IN NI-BASED SUPERALLOYS BY NEUTRON DIFFRACTION

Yan Chen, Ke An, Alexandru D. Stoica

May 11th, 2020

Prepared by
OAK RIDGE NATIONAL LABORATORY
Oak Ridge, TN 37831-6283
managed by
UT-BATTELLE, LLC
for the
US DEPARTMENT OF ENERGY
under contract DE-AC05-00OR22725

CONTENTS

LIST OF FIGURES

LIST OF TABLES

ACRONYMS

LD	Longitudinal direction
ND	Normal direction
ORNL	Oak Ridge National Laboratory
RT	Room temperature
SNS	Spallation Neutron Source
TC	Thermocouple
TD	Transverse direction
TOF	Time-of-flight

PREFACE

The residual stress and its relaxation in critical engineering components are key to structural materials reliability. The determination of residual stress in bulk engineering structures like Ni-based superalloys can be conducted by measuring the lattice strain with penetrating neutron diffraction. The state-of-the-art engineering diffraction beamline VULCAN at the Oak Ridge National Laboratory (ORNL) Spallation Neutron Source (SNS) provides the critical capability to evaluate the residual strain/stress relaxation in engineering component thanks to the high flux and event data features. By the means of residual stress/strain calculation, it is critical to accurately determine the stress-free lattice spacing d_0, which can be altered by the change of chemistry, unrelieved stress, and measurement scheme. Here we reported d_0 determination for determining residual stress relaxation and distribution in Alloy 718 superalloys after different quenching treatments. Selection of locations for d_0 measurement was discussed by considering the neutron path, attenuation and sample alignment. A dynamic d_0 that resulted from atom diffusion and chemistry change was estimated as function of time for the *in-situ* relaxation characterization. It demonstrated how the dynamic d_0 values may influence on the strain calculation in different thermally treated samples. The results highlight the importance of dynamic d_0 for *in-situ* relaxation involving chemical changes and provide guidance to the dynamic d_0 measurement and simulation.

ACKNOWLEDGMENTS

This research used the Spallation Neutron Source at the Oak Ridge National Laboratory, which is a DOE Office of Science User Facility. We thank Harley Skorpenske and Matt Frost for their technical support of neutron experiment.

1. INTRODUCTION

1.1 LATTICE STRAIN MEASUREMENTS BY TIME-OF-FLIGHT NEUTRON DIFFRACTION

Lattice strain due to residual applied stress can be measured by diffraction technique. The benefit of neutron's deep penetration into materials allows lattice strain measurement inside an engineering structure while it either contains residual stress or under applied stress. Below are fundamentals of the technique by using time of flight neutron source such as the Spallation Neutron Source at Oak Ridge National Laboratory. Further details can be found in the book by M.T. Hutchings et al [1].

The principle of strain measurements by neutron diffraction is based on Bragg's law,

$$\lambda = 2d_{hkl}\, sin\, \theta_B \tag{1}$$

where λ is the neutron wavelength, d_{hkl} the interplanar spacing of the (*hkl*) family of lattice planes, and $2\theta_B$ the angle between the incident and diffracted neutron beams. For time-of-flight (TOF) neutrons with a wide energy range, according to de Brogile's law, the detected neutron wavelength is determined from its TOF (t),

$$\lambda = \frac{h}{mv} = \frac{h}{mL}t \tag{2}$$

where *h* is Planck's constant, *m* the neutron mass, *v* the neutron velocity and *L* the flight path from the moderator to the detector. Thus, in a TOF spectrum of a material, the *d*-spacing is obtained from the position t_{hkl} of the Bragg peak,

$$d_{hkl} = \frac{h}{2mL\, sin\, \theta_B}\, t_{hkl} \tag{3}$$

When the material is subjected to an applied stress, the diffraction peak will shift to a different time, and hence *d*-spacing (d_{hkl}). From the change in peak position, the (*hkl*)-specific lattice strain can be determined as

$$\varepsilon^{hkl} = \frac{d_{hkl} - d_{0,hkl}}{d_{0,hkl}} \tag{4}$$

where $d_{0,hkl}$ is the stress-free lattice spacing. Thus, the interplanar spacing (d_{hkl}) constitutes an intrinsic strain gauge for the material.

The measured lattice strain represents the component of the strain tensor along the direction of the momentum transfer *Q*, which bisects the incident and diffracted beams. A complete definition of the strain tensor requires measuring at least six non-coplanar directions. In the simplified case with a given orthogonal coordinate system (not necessary to correspond to the principal axes), measuring the three normal lattice strains is sufficient to determine the three normal stress components, regardless of the measurement of the shear components.

1.2 STRESS CALCULATION FROM THE MEASURED LATTICE STRAINS

As an analog of Hooke's law, the stress tensor (σ_{ij}) (normal stresses) can be calculated from the strain tensor (ε_{ij}),

$$\sigma_{ij} = \frac{E^{hkl}}{(1+\nu^{hkl})}\left\{\varepsilon_{ij}^{hkl} + \frac{\nu^{hkl}}{(1-2\nu^{hkl})}\left(\varepsilon_{11}^{hkl} + \varepsilon_{22}^{hkl} + \varepsilon_{33}^{hkl}\right)\right\} \quad (5)$$

where i,j=1,2,3 indicate the components relative to three orthogonal axes. Eq. (5) indicates that any three orthogonal stress components can be determined from the corresponding orthogonal strain components. E^{hkl} and ν^{hkl} are "diffraction elastic constants". They are linear calibration constants which relate the macroscopic stress in the sample to the lattice strains for a given crystallographic [*hkl*] direction. The diffraction elastic constants can be measured from calibration experiments in which a polycrystalline sample is subjected to known uniaxial loading. Eq. (5) can be simplified with a known symmetry of residual stress/strain state, which is used for the experiment summarized here during *in-situ* residual stress relaxation.

1.3 STRESS-FREE LATTICE SPACING $D_{0,HKL}$ FOR RESIDUAL STRESS CALCULATION

A correct choice of stress-free lattice spacing $d_{0,hkl}$ is of importance to accurately determine the lattice strain (Eq. (4)) and thus the residual stress. In stable and homogeneous samples, a constant $d_{0,hkl}$ is used, and its measurement is straightforward. There are some approaches that are widely used to prepare the stress-free sample. One concept is to reduce sample dimensions so that the macro stress cannot be built up. For examples, grinding the sample into fine powders; cutting out a small volume from the sample, which usually matches the neutron gauge volume; and, comb-cutting the sample to have small portions with at least two dimensions reduced. In addition, if sample destruction is avoided, the location near the sample corner can be considered as a stress-free sample. Another concept is to relieve the residual stress in the original sample, and a full annealing is typically used. It is still worth noting that the stress mentioned is in macro scale, which is usually considered in engineering applications. The stress and strain in micro scale may not be fully eliminated in those stress-free samples, for example, local stress/strain near a dislocation within a crystallite. The micro stress is usually out of the scope of residual stress measurement for engineering applications, and it is also hard to quantify via the diffraction approach.

In chemically inhomogeneous samples, such as weldment, nearly all aluminum alloys and additive-manufactured samples, the lattice spacing at stress-free states could be location-specific. A chemistry- and geometry-identical sample that has stress relieved (d_0 sample) is recommended to measure $d_{0,hkl}$ at the desired locations. The d_0 sample can be comb-cut to relieve the residual stress. An appropriate annealing may be chosen only if the chemistry does not change during the high temperature treatment. In some special case, the measurement of d_0 can be waived if an additional constraint of stress or strain is applied to Eq. (5), and therefore, the preparation of stress-free sample is not required. Taking a thin-wall sample as an example, the plane-stress approximation can be applied, so that the stress at normal direction (along the thickness) is zero, i.e. $\sigma_{yy} = 0$. Applying this constraint, one will calculate the other normal stress components in Eq. (5) without an input of d_0 value [2].

For the *in-situ* residual stress/strain relaxation measurement in this study, the chemistry of the sample is changing over annealing time during the isothermal dwell at the high temperature. As the stress-free lattice spacing is also expected to evolve with the chemistry, a static $d_{0,hkl}$ will not be applicable for *in-situ* measurement. The dynamic $d_{0,hkl}$ values thus need to be determined, however, attentions were seldom paid to this correction [3]. In this study, we will demonstrate a simple model to estimate the dynamic $d_{0,hkl}$ in Ni-base superalloy due to atom diffusion and chemical changes at high temperature, and indicated the d_0 effects on the lattice strain calculation during the relaxation.

2. EXPERIMENTS

2.1 EXPERIMENTAL BASICS ON VULCAN

The lattice strain measurement was done at the VULCAN engineering materials diffractometer at the Spallation Neutron Source, the Oak Ridge National Lab [4,5]. The schematic of the instrument layout and residual stress setup is shown in Figure 1, where a small volume in red is determined by the incident slit and the receiving collimators. Two lattice d-spacings are measured (in Q_1 and Q_2) into the ±90° banks. The third direction Q_3 (normal to the paper) is measured after rotating the sample 90° along the Q_2 direction. Three strain components in Q_1, Q_2 and Q_3 direction are needed for residual stress calculations. The incident silts and receiving collimators are used to define the neutron gauge volume. With consideration of significant attenuation in the large bulk sample, a large gauge volume was used to improve the statistics in the *in-situ* relaxation measurement, i.e. 5×5 mm^2 incident slits opening along with 5 mm receiving collimators. In the static measurement of d_0 and residual stress map, the vertical opening of incident slit was slightly reduced to 4 mm (5×5×4 mm^3 gauge volume) in order to improve the spatial resolution along *Z* direction and increase the number of data points in the map. The Ni (311) peak which is the least affected by intergranular stress is used to determine the strain in the bulk. The chopper setting of 60 Hz with a band center 0.19 nm was used, and the counting time for each measurement was determined based on the collected intensity. For *in-situ* measurement, neutrons were collected continuously and then sliced based on good statistics to yield a small fitting statistics error. The data is analyzed by single peak fit using the VDRIVE software [6].

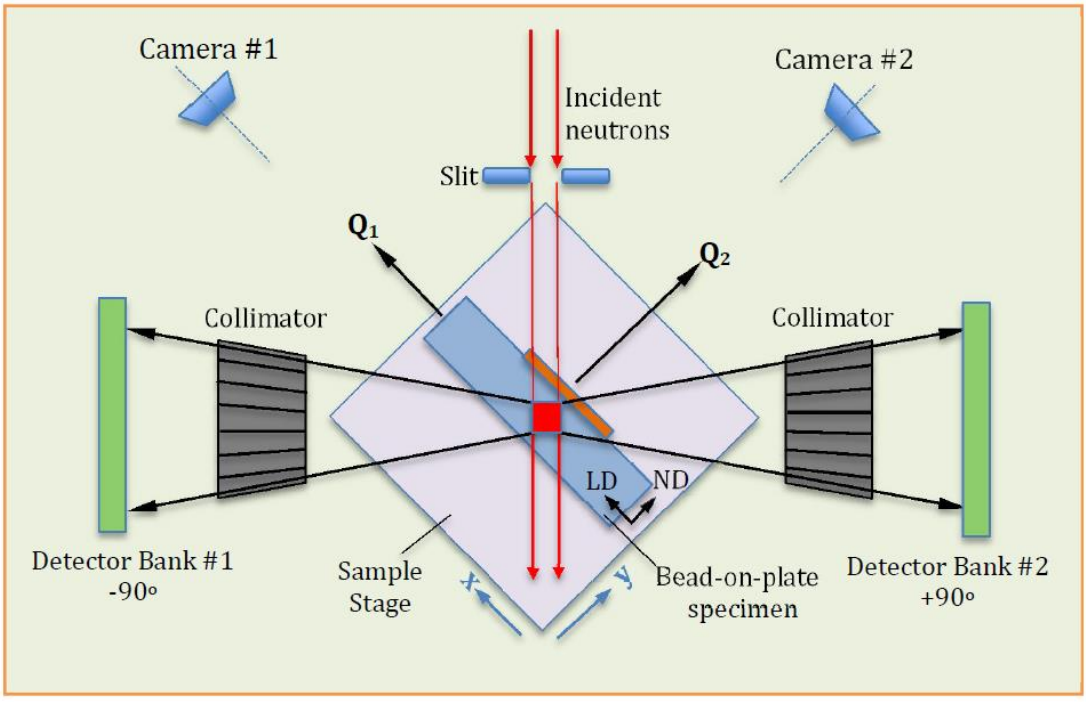

Figure 1. Schematic illustration of the bead-on-plate experimental set-up on VULCAN (top view, not to scale). The -90° and +90° detector banks record diffraction peaks of the (*hkl*) lattice planes whose normals are parallel to Q_1 and Q_2, respectively. Strain components along these two directions are measured simultaneously. The bead-on-plate sample is positioned on top of the sample stage and aligned at 45° from the incident beam. (cited from [7]).

2.2 SAMPLES

Commercial Alloy 718 samples are prepared in this study, and the list of samples selected for the investigation is shown in Table 1. All the samples (76×27×27 mm^3) were quenched from solid solution treatment above δ phase solvus temperature by either dropping to water or oil. After quenching, a typical double precipitation ageing treatment was carried out as 8 hours isothermal dwell at 718°C, then furnace cool to 621°C for another 8 hours dwell, and finally air cool to room temperature. Sample 1H and 2HOQ are a pair which were quenched by water and oil, respectively. Sample 1HWQAGE and 1HOQAGE are a pair which were double aged after quenched by water and oil, respectively. All samples were cut from 76 mm long bars for contour residual stress measurements by the other vendor. The longer part (44×27×27 mm^3) of each sample was selected for the *in-situ* residual strain relaxation measurements by annealing, and the residual strains before and after residual stress relaxation were investigated as well. The calculation of residual stress relaxation and mapping will be reported elsewhere.

Table 1. Sample list of the Ni-based Alloy 718 supper alloy investigated by neutron diffraction.

Sample	Quench	Age
1H	Water	No
2HOQ	Oil	No
1HWQAGE	Water	Yes
1HOQAGE	Oil	Yes

2.3 MEASUREMENT OF STRESS-FREE LATTICE SPACING D_0

To perform the *in-situ* residual stress relaxation, the location of peak residual stress inside the samples was selected. The location is determined by initial residual stress distributions measurement along selected lines (the details of the result will be reported elsewhere). The locations of residual stress before and after residual stress relaxation in the provided samples are shown in Figure 2. Considering the symmetry of the residual stress distribution, it is rational to assume the stress/strain components along *X* (normal direction or ND) and *Z* (transverse direction or TD) directions are same at the center lines along *Y* (longitudinal direction or LD) direction, and the distributions of residual stress along ND and TD are same.

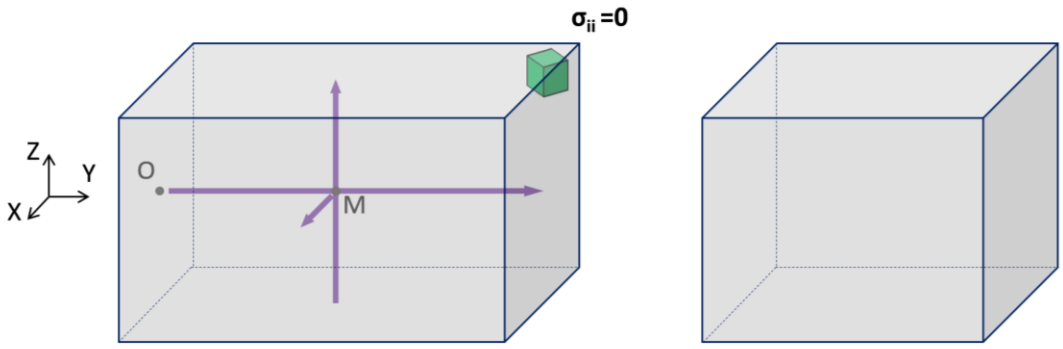

Figure 2. Schematic view of measurement locations of residual stress and d_0. The green cube indicates the neutron gauge (5×5×4 mm^3) volume at d_0 measurement.

To determine the d_0 values of each sample at room temperature, the lattice spacing at selected locations were measured and compared. During the quenching, the residual stress built up due to the uneven cooling rate through the bulk (e.g. fast near outside). At the location near a corner of the sample bar, the stresses near surface are close to 0 because no constraints in the three directions and the cooling rate is relative uniform thanks to the relatively small volume at the corners. We took that kind of locations as a stress-free sample for each measured bar. The choice of the four corners is shown in Figure 3. The center of the gauge volume was about 4 mm in from the sample surfaces nearby. Due to the sample geometry, the neutron paths were different from one to other. Therefore, the neutron attenuation occurred when the diffracted beam went through the sample (dashed arrow in Figure 3). The diffracted beams at Location A and B are free of attenuation, while there is attenuation at the LD direction for Location C and D by using the detector Bank 1. Additionally, since the samples were layered on the others at the d_0 measurement, the neutron paths and attenuations were slightly different in the top and the bottom samples at the out-of-plane directions due to using the wide-area detectors. In addition to utilizing the sample corners, a 3×3×3 mm^3 cube was cut out from the center of the cutting surface of selected samples, shown as Location E in Figure 3 (Right). The measured d_0 values via different locations were compared.

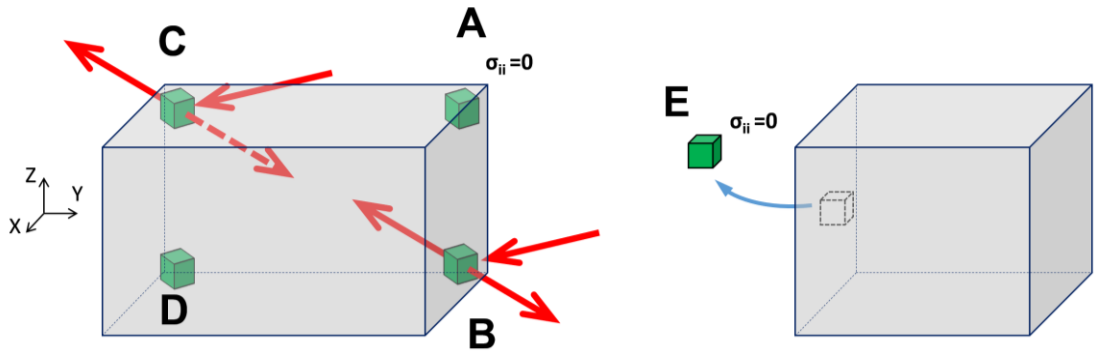

Figure 3. Locations of the d_0 measurement. The red arrows show the examples of the neutron paths, and the dashed line shows the occurrence of neutron beam attenuation.

Special cautions are taken for calculating the stress-free d_0 at the elevated temperature. At the elevated temperature, the d_0 is calculated by compensating the change of lattice parameter due to thermal expansion. Considering the possible temperature difference at center and corner (corner temperature could be slightly lower due to heat loss), the uniform change of lattice parameter due to heating from room to the elevated temperature is measured at the measurement location (Point M in Figure 2 (Right)) during *in-situ* residual stress relaxation. The measurement was carried out on 2HOQ, 1HOQAGE and 1HWQAGE samples. The d_0 calculated above is the value at the end of the isothermal dwell. The dynamic values during the dwell were estimated by using a simple math model that was validated with the reported experimental data of d_0 evolution.

2.4 THE *IN-SITU* SETUP FOR RESIDUAL STRESS RELAXATION MEASUREMENTS

The sample bar was held in the VULCAN MTS loadframe with a slight compressive stress of -0.3 MPa by two alumina grips, and an induction coil was used to rapidly heat up the sample bar. It was difficult to directly measure the internal temperature at the neutron gauge volume in such a bulk sample. Two thermocouples were applied to monitor two surface temperatures at the measurement location. The one at the front surface was used to control its temperature reading at 719.5°C during the *in-situ* relaxation. The other one at the bottom surface was for monitoring purpose. The setup is shown in Figure 4. A 5×5×5 mm^3 gauge volume was used during the relaxation measurement. The -90° and +90° detector banks recorded diffraction peaks in real time along the LD and ND directions, respectively. The orthogonal

lattice strain components were calculated correspondingly. With the symmetry assumption, the three orthogonal stress components were calculated and reported elsewhere.

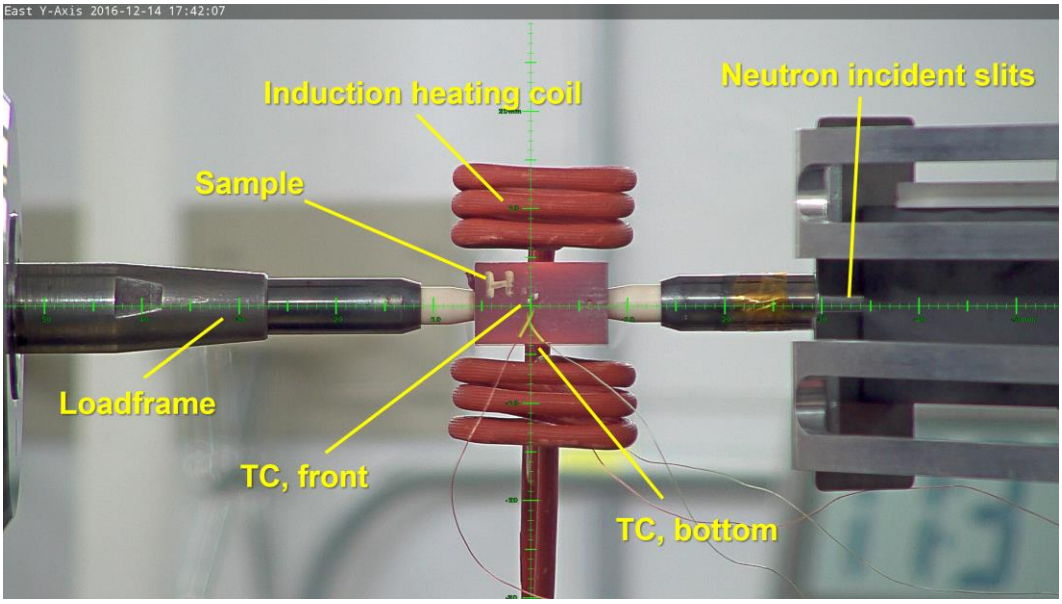

Figure 4. The *in-situ* residual stress relaxation setup on VULCAN. (TC is abbreviation of thermocouple).

3. RESULTS

3.1 SELECTION OF $D_{0,311}$ FOR RESIDUAL STRESS MAPPING AT ROOM TEMPERATURE

The $d_{0,311}$ values which were measured at different locations by both detector banks are shown in Figure 5. Some of the values have significant discrepancy between each other, which may be contributed by multiple reasons. First, the neutron path and attenuation show influence of $d_{0,311}$ measurement. As shown in Figure 3, the attenuation of the diffracted beam occurred at LD direction of Location C and D. As one can see in Figure 5, the measured $d_{0,311}$ values show larger discrepancies at Location C and D along LD. In contrast, the values at Location A and B along LD, and at Location A, B, C and D along ND/TD, which are less affected by neuron attenuation, are more consistent. Therefore, the discrepancy exhibits correlations to the neutron path. Theoretically, the attenuation would not shift the *d*-spacing, but it may influence the measurement indirectly. For examples, low statistics increasing the fitting error, and severe shadowing on the wide detector bank altering the detector alignment. A comprehensive study on the attenuation is out of the scope of this document. It is rational to exclude the measurement points where the neutron paths are significantly different (Location C and D of all samples, and the Location A or B of a sample which was layered at the top or bottom during the measurement), in order to minimize the influence. Second, unexpected inhomogeneous chemistry and composition in the sample can shift the lattice *d*-spacing. It may be one of the reasons for the small fluctuation of $d_{0,311}$ values at various locations. However, it is costly and not worthwhile to figure out the spatial dependence of $d_{0,311}$ since the fluctuation is not significant and not intentionally designed. Doing average of those selected is an appropriate approach. Third, differences are observed between the values along LD (using detector bank 1) and along ND/TD (using detector bank 2). It can be caused by the slight misalignment between those two banks. It can also be resulted from the fact that the stresses were not fully relieved at those locations near the corner. In particular, the complex phase compositions in Alloy 718 superalloy may hold complementary interphase stresses while showing a balance at the macro scale. Nevertheless, those measured *d*-spacing values are the best approximation of those at the stress-free state. Using the bank-specific (direction-specific as well) d_0 value for the subsequent calculation will thus not to add up the error due to the bank (and directional) discrepancy. The absolute strain/stress values that are calculated by using them may show slight shift from the true values, but it will reflect the same trend in the mapping and *in-situ* relaxation.

Therefore, to minimize the influence discussed as above at the determination of $d_{0,311}$, the data points marked with "∇" in Figure 5were used and averaged for $d_{0,311}$ of each specimen. The $d_{0,311}$ values measured at Location E that was a small cube cut from the specimens are also compared in Figure 5. The observed inconsistency may be attributed to the chemistry/composition discrepancy and/or the sample alignment. Because the 3×3×3 mm^3 cube dimension is small, a rocking curve was scanned and fitted with Gaussian function to determine the sample position, which was different from the visual alignment the sample corners via the camera. The TOF neutron diffraction is sensitive to the sample position, and thus even small displacement from the beam center may affect the measured d_0 value. With considerations above and the comparison in Figure 5, the value measured at Location E was not used to calculate $d_{0,311}$.

In Figure 5 the $d_{0,311}$ values of different samples are compared. The values of 1H and 2HOQ specimens before relaxation are significantly larger than those of aged specimens and the values of relaxed specimens, which indicates the change of chemical composition or phase composition in response to the thermal treatment history and the relaxation in this work. In addition, the measured $d_{0,311}$ values along LD and ND/TD are consistent in all the specimens except in 1HOQAGE and 1HWQAGE after relaxation. In those two specimens, $d_{0,311}$ is measured to be larger at LD than at ND/TD.

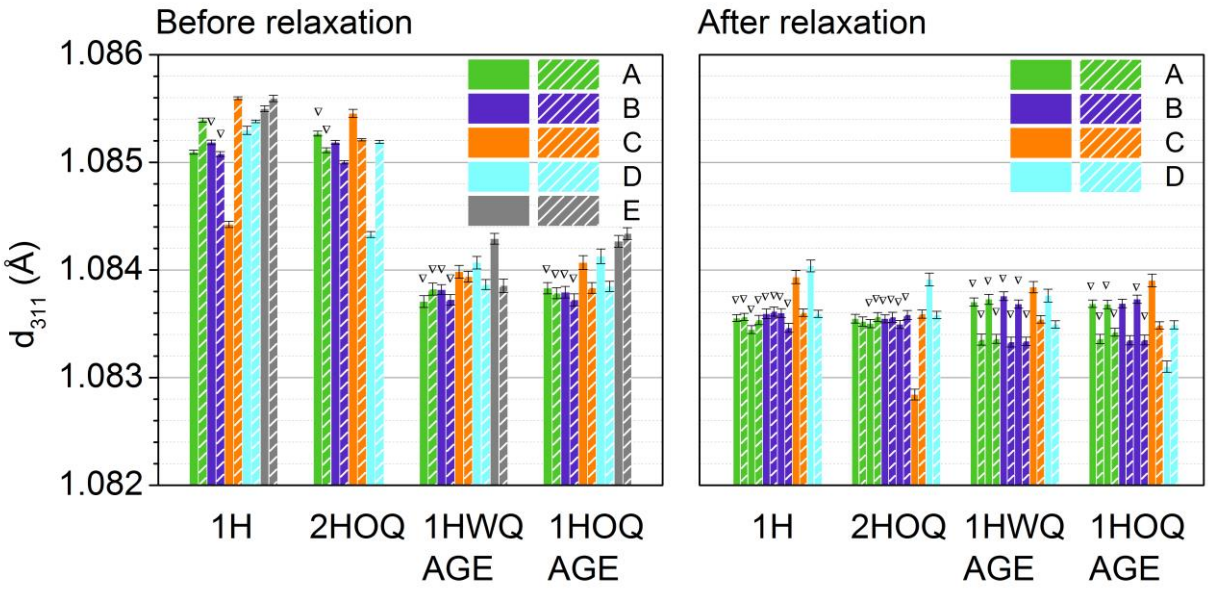

Figure 5. The measured d_0 values of (311) peak at different locations at the specimens. The solid bars show the measurement at LD while the strip bars show the measurement at ND/TD. The colors show indicate the locations of measurement, and the location symbols coresspond to those in Figure 3. The values with ∇ mark are used to determine $d_{0,311}$.

3.2 DETERMINATION OF DYNAMIC $D_{0,311}$ VALUES FOR *IN-SITU* STRAIN CALCULATION DURING THE RESIDUAL STRESS RELAXATION AT HIGH TEMPERATURE

The induction heating coil was used for *in-situ* relaxation, as shown in Figure 4. Under the electromagnetic field, the top and the bottom surfaces of the sample acted as the heat source. There was not a heat sink in the internal bulk. The heat mainly transported to the air through the other sample surfaces while some was dissipated via radiation. As the alloy is a good thermal conductor, the neutron gauge volume inside the bulk is expected to quickly reach the steady state. Therefore, in the *XZ*-cross-section including M point, the center of bottom (or top) surface and the center of front (or back) surface are the two extremes of the temperature distribution near the neutron gauge volume, which are measured by the two thermocouples, respectively. In Figure 6, the temperature readings of the two thermocouples during relaxation are shown, taking 1H sample as an example. The reading at the front surface was close to the set point 719.5°C during the relaxation. The reading at the bottom surface was about 723.5°C at the beginning. Then it decreased to about 722°C within 2 hours and maintained at this temperature as a steady state. The max difference between the two readings were smaller than 4°C. Assuming the coefficient of thermal expansion of Ni superalloy is typically about 15×10^{-6} °C^{-1}, the temperature fluctuation would bring a thermal strain variation about 60×10^{-6}. It is negligible compared to the lattice strain change due to the relaxation, as what will be discussed in the following. Therefore, the temperature reading 719.5°C at the front surface will be used as the nominal temperature.

The stress-free lattice spacing at high temperature was calculated using the value at room temperature measured as above and considering the lattice thermal expansion. The thermal expansion was measured from the cooling curves of lattice spacing at the measurement point (Point M in Figure 2) after the *in-situ* relaxation. After the longtime of annealing, the material trended to the equilibrium, and further chemical change that may alter the lattice spacing unlikely occurred at cooling. Therefore, the lattice spacing changes before and after cooling are caused by the real thermal expansion. Figure 7 shows the evolution of thermal strains (calculated using (311) lattice spacing) at 2HOQ, 1HOQAGE and 1HWQAGE samples

during cooling. The curves exhibit highly similar trend in all sample along both of LD and ND (by detector Bank 1 and detector Bank 2, respectively). When the data of the three samples are plotted in the same figure (taking LD data as the example), the thermal expansions are highly overlapped. Therefore, the pre-treatments did not significantly alter the thermal expansion behavior of the superalloy samples. A single thermal expansion value will be calculated and applied to all samples. The results were calculated as listed in Table 2. Quantitatively, those values are highly consistent for all the measured samples. The average thermal expansion of 1.158% is used to calculate $d_{0,311}$ at 719.5°C from the $d_{0,311}$ measured at RT for all samples along both LD and ND. Apparently, this stress-free $d_{0,311}$ values are applicable to the end of the annealing (denoted as $d^{e}_{0,311}$), and their dynamic changes during annealing will subsequently be estimated in the following.

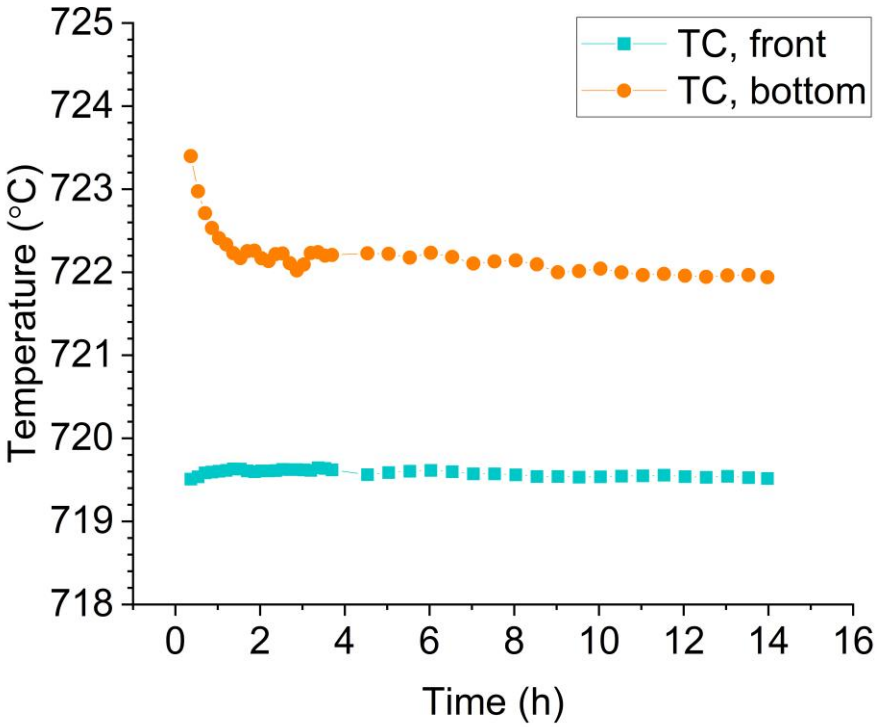

Figure 6. Temperature readings of the two thermocouples (TC) at the 1H sample front surface and bottom surface, respectively, during the *in-situ* residual stress relaxation.

The lattice parameter drift due to the chemistry changes during the isothermal dwell at 719.5°C is determined phenomenologically. The time dependence is assumed to obey the function as the following.

$$d_0 = Ae^{-t/\tau} + C \tag{6}$$

where d_0 is the stress-free d-spacing in Å, t is the time of dwell in minute, and A, τ and C are the coefficients to be determined.

In the reference [8], it is reported that the lattice parameter of Alloy 718 superalloy evolves during stress-free ageing at 720°C. The experimental data are well fit with the Eq. (6), shown in Figure 8(Left), and the coefficients are determined as A = 0.00204 Å, τ = 104.802 min and C = 3.64334 Å for the lattice constant. The sample and the isothermal dwell condition in this study is highly similar with those in the

reference [8], and therefore, the above determined parameters will be used to estimate the d_0 drift of (311) peak during the *in-situ* relaxation. The time dependence is

$$d_{0,311} = \frac{A}{\sqrt{11}} e^{-t/\tau} + C_1 \tag{7}$$

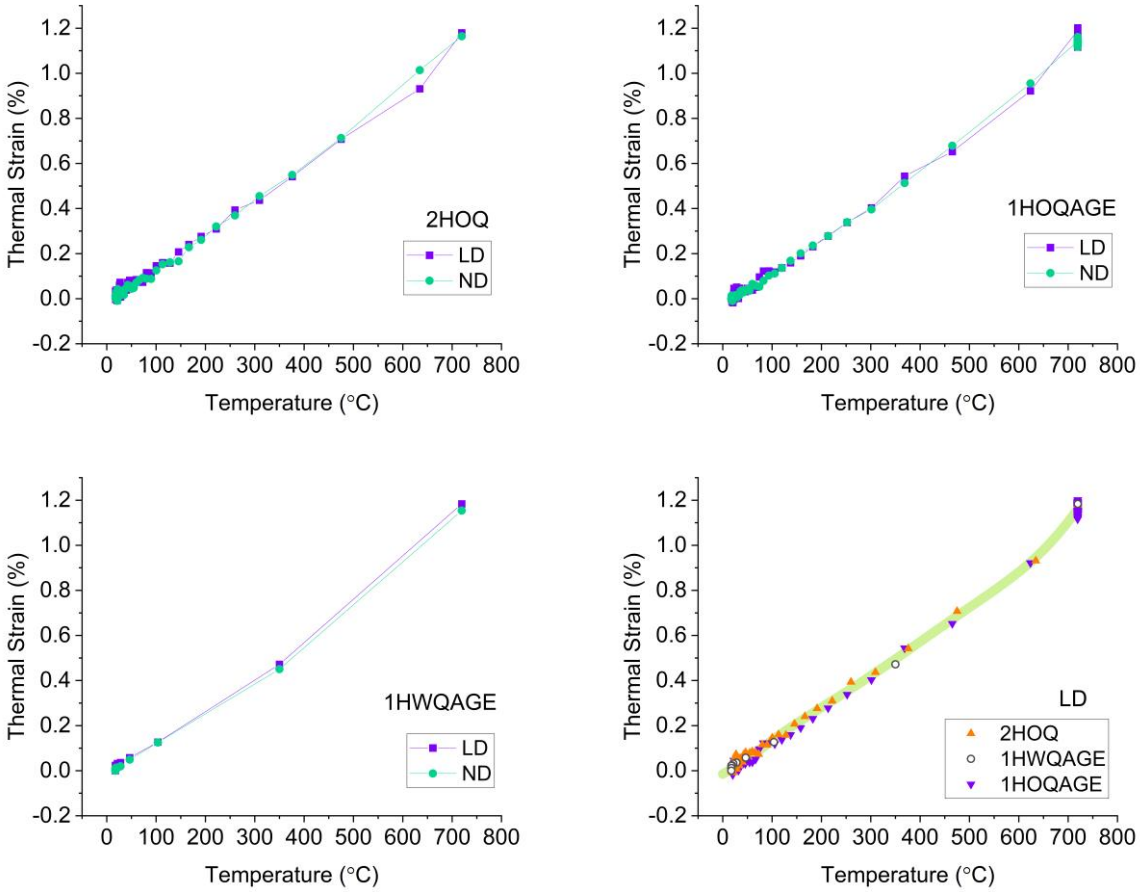

Figure 7. The lattice thermal strains by (311) peak during cooling down from 719.5°C to room temperature in selected samples

Table 2. Thermal expansion of specimens from room temperature (RT) to 719.5°C

Specimen	$\frac{d_{0,311}(719.5°C) - d_{0,311}(RT)}{d_{0,311}(RT)}$	
	Detector Bank 1	Detector Bank 2
2HOQ	0.01171	0.01159
1HWQAGE	0.01168	0.01146
1HOQAGE	0.01162	0.01140
Average	0.01158	

The parameters A and τ that determine the curve shape will use the same values as determined above for Eq. (6). The coefficient $\sqrt{11}$ is from the ratio between the unit cell lattice constant a and the (311) lattice spacing. The parameter C_1 in Eq. (7) may not agree with C in Eq. (6) due to the systematic error from different instruments. To eliminate the influence on C_1 variation, the calculated $d^e_{0,311}$ value along with the relaxation ending time t_e is used as input, and it thus follows:

$$d^e_{0,311} = \frac{A}{\sqrt{11}} e^{-t_e/\tau} + C_1 \tag{8}$$

Therefore, solving Eq. (7) and Eq. (8), the dynamic $d_{0,311}$ is calculated by

$$d_{0,311} = d^e_{0,311} + \frac{A}{\sqrt{11}}\left(e^{-t/\tau} - e^{-t_e/\tau}\right) \tag{9}$$

The Eq. (9) will be directly applied to $d_{0,311}$ calculation in the quenched samples 1H and 2HOQ. For the aged samples 1HWQAGE and 1HOQAGE, the ageing history shall be considered. The time will be shifted by 8 hours in according to the pre-ageing at 718°C for 8 hours, while the second age at the lower temperature 621°C is not considered to bring more significant change of chemistry.

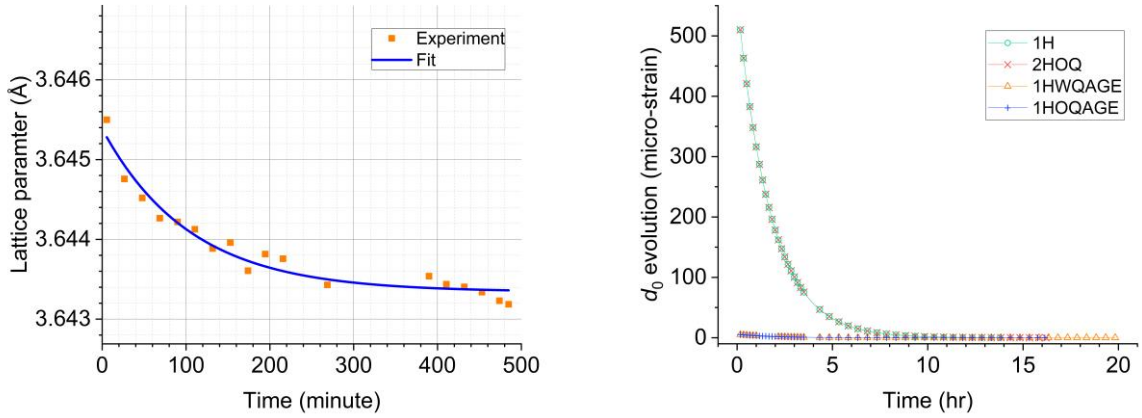

Figure 8. Dynamic stress-free lattice spacing in Alloy 718 at high temperature. (Left) Fitting the lattice parameter drift during relaxation using the experimental data reported in the reference [8]. (Right) Calculated d_0 evolution in the samples at isothermal dwell at 719.5°C in this study.

Figure 8(Right) shows the calculated d_0 evolution of all samples in the form of strain, which reference is selected as the equilibrium at time equaling to infinity. It clearly shows that the major changes of d_0 are occurring at the first 8 hours of annealing in the as-quenched samples. The subsequent changes of d_0 in the rest of annealing or in the aged samples are not that significant. As a result, using a constant d_0 to calculate residual strain/stress may be valid for the aged samples, but the dynamic d_0 correction is essential for the calculation with severe chemical changes in the as-quenched samples in the at least first 8 hours. As well, the results support assumption not to consider the second ageing at 621°C to estimate the dynamic d_0 values in aged samples.

3.3 THE EFFECT OF D_0 ON *IN-SITU* RESIDUAL STRAIN CALCULATION

In the following *in-situ* residual stress relaxation experiment, the volume locating at (X,Y,Z) = (0, 20, 0), which is representative and has relatively high initial residual stress, is selected. The kinetics of the

residual strain relaxation along LD and ND at 719.5°C were plot in Figure 9. The strains calculated using constant $d^e_{0,311}$ and dynamic $d_{0,311}$ are plotted in the same figure for comparison.

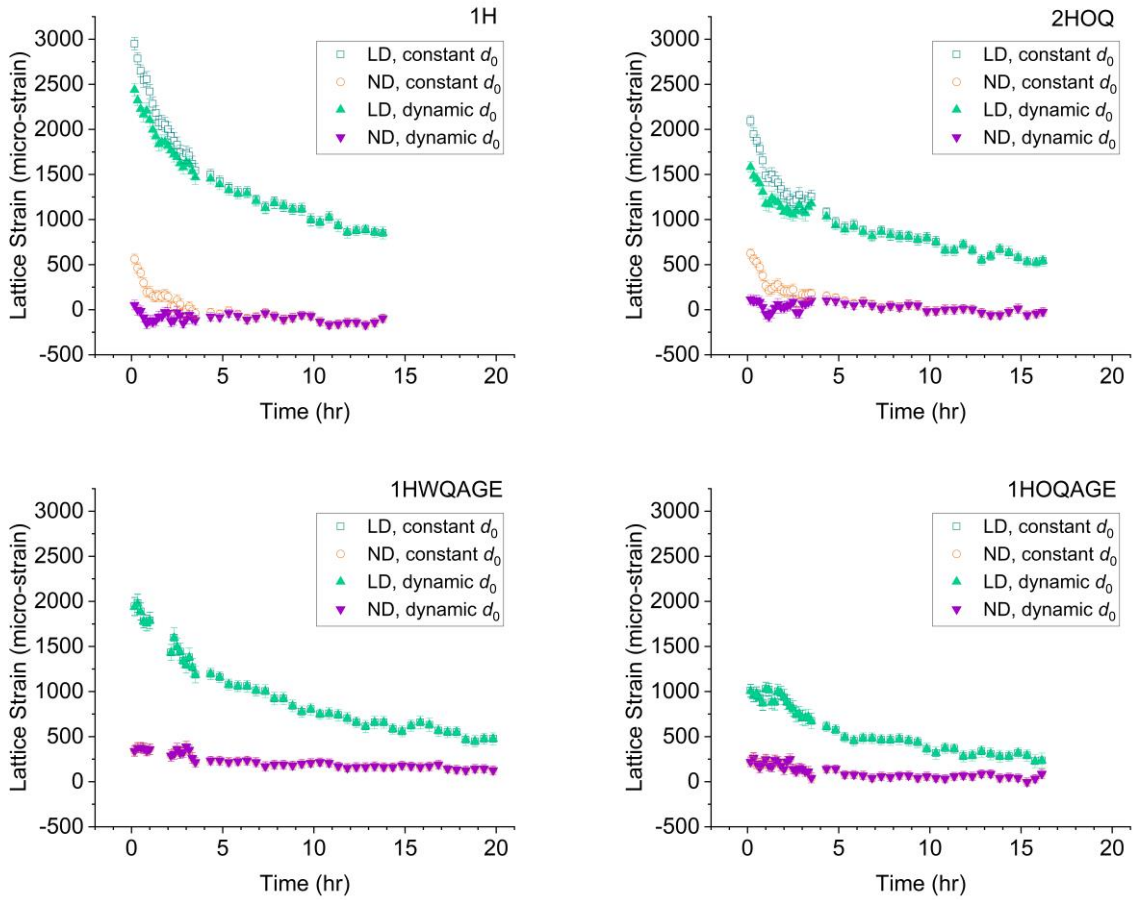

Figure 9. Comparison of the calculated lattice strains using constant d_0 and dynamic d_0 during *in-situ* residual stress relaxation in the four cut samples.

As what are visualized in Figure 9, the effect on dynamic $d_{0,311}$ agrees with the prediction from Figure 8 (Right). With the correction of dynamic $d_{0,311}$, the calculated strains along both LD and ND are significantly reduced at the first 8 hours of annealing in as-quenched samples 1H and 2HOQ, in comparison to the results with static $d_{0,311}$. Particularly, the reduction is severe at the first 3 hours. It is interesting that the strains along ND show a similar trend with those along LD while with lower magnitude if calculated with constant $d^e_{0,311}$; in contrast, with dynamic $d_{0,311}$ correction, the change of ND strains is compensated, and they show nearly no change, close to zero. After 8 hours, the difference of strains with static and dynamic $d_{0,311}$ becomes subtle. In the aged samples 1HWQAGE and 1HOQAGE, there is almost no difference in either LD strain or ND strain with dynamic $d_{0,311}$ correction, except slight decreases at the beginning of annealing.

Based on the results with dynamic d_0 in Figure 9, in the 1H and 2HOQ samples, which are without ageing, the residual strains along LD rapidly decrease in the first 2 hours, and a large magnitude of residual strains are released in this period. In the subsequent 10+ hours, although the relaxation continues, the rate becomes much lower. After the 14-16 hours relaxation, the system still did not reach the equilibrium, but the changes were slowed down significantly. In contrast, the ageing process changes the

relaxation behaviors. In 1HWQAGE and 1HOQAGE samples, the residual strains do not quickly reduce. Especially in 1HOQAGE, which is oil-quenched and aged, the residual strains changed little at the beginning, and the significant relaxation seems to start after 2 hours dwell at 719.5°C.

As for result of the relaxation at 719.5°C for 14-20 h, the residual strains have been significantly relieved along LD. The quenched samples 1H and 2HOQ kept nearly zero strain along ND throughout the relaxation process. The aged samples 1HWQAGE and 1HOQAGE have slightly higher strains along ND at the beginning and gradually reduced towards zero at the annealing. The residual stresses of all samples would exhibit similar trends, and the calculated results will be reported elsewhere.

4. SUMMARY

Using the engineering diffractometer at the high flux spallation neutron source as a great tool for characterizing the residual stress/strain relaxation in structural material, we demonstrated that the determination of dynamic d_0 at high temperature implemented in this practice is proved feasible. The neutron path, attenuation and sample alignment need to be considered for choosing location for the d_0 measurement of bulk sample at room temperature. The stress-free lattice spacing d_0 at high temperature can be reasonably calculated from the room temperature measurement by compensating the thermal expansion that was characterized via *in-situ* neutron diffraction. The d_0 evolution during annealing at high temperature due to interphase atom diffusion and chemistry change was found to impact the residual strain calculation significantly. The dynamic d_0 values as a function of time were estimated via a simple empirical model and fitting to experimental data. The influence deviated with different previous thermal treatments. The results provide important guideline of consideration for the stress relaxation characteristics of the superalloy samples, which provides essential benchmark for finite element modeling of the process.

5. REFERENCES

1. M.T. Hutchings, Introduction to the Characterization of Residual Stress by Neutron Diffraction, Taylor & Francis Group, 2005.
2. K. An, L. Yuan, L. Dial, I. Spinelli, A.D. Stoica and Y.F. Gao, Neutron Residual Stress Measurement and Numerical Modeling in A Curved Thin-Walled Structure by Laser Powder Bed Fusion Additive Manufacturing, *Materials and Design*, 135, 122–132, 2017.
3. P.E. Aba-Perea, T. Pirling and M. Preuss, In-situ Residual Stress Analysis during Annealing Treatments Using Neutron Diffraction in Combination with A Novel Furnace Design, *Materials and Design*, 110, 925–931, 2016.
4. K. An, H.D. Skorpenske, A.D. Stoica, D. Ma, X.L. Wang and E. Cakmak, First in situ Lattice Strains Measurements under Load at VULCAN, *Metallurgical and Materials Transactions A*, 42, 1, 95–99, 2011.
5. K An, Y. Chen and A.D. Stoica, VULCAN: A "Hammer" for High-Temperature Materials Research, *MRS Bulletin*, 44, 11, 878–885, 2019.
6. K. An, VDRIVE – Data Reduction and Interactive Visualization Software for Event Mode Neutron Diffraction, ORNL Report, ORNL-TM-2012-621, Oak Ridge National Laboratory, 2012.
7. K. An, D.A. McClintock and M. J. Frost, Residual Stress Measurements of Front Window Welds in A Prototypical Spallation Neutron Source Target Module, ORNL Report, ORNL-TM-2018-837, Oak Ridge National Laboratory, 2018.
8. H. Qin, Z. Bi, D. Li, R. Zhang, T.L. Lee, G. Feng, H. Dong, J. Du and J. Zhang, Study of Precipitation-Assisted Stress Relaxation and Creep Behavior during the Ageing of A Nickel-Iron Superalloy", *Materials Science and Engineering A*, 742, 493–500, 2019.